

Cite this: *Chem. Sci.*, 2021, 12, 632

All publication charges for this article have been paid for by the Royal Society of Chemistry

Cooperative activating effects of metal ion and Brønsted acid on a metal oxo species†

Gui Chen,^a Li Ma,^b Po-Kam Lo,^c Chi-Keung Mak,^{*c} Kai-Chung Lau^{id} ^{*c} and Tai-Chu Lau^{id} ^{*c}

Metal oxo (M=O) complexes are common oxidants in chemical and biological systems. The use of Lewis acids to activate metal oxo species has attracted great interest in recent years, especially after the discovery of the CaMn₄O₅ cluster in the oxygen-evolving centre of photosystem II. Strong Lewis acids such as Sc³⁺ and BF₃, as well as strong Brønsted acids such as H₂SO₄ and CF₃SO₃H, are commonly used to activate metal oxo species. In this work, we demonstrate that relatively weak Lewis acids such as Ca²⁺ and other group 2 metal ions, as well as weak Brønsted acids such as CH₃CO₂H, can readily activate the stable RuO₄⁻ complex towards the oxidation of alkanes. Notably, the use of Ca²⁺ and CH₃CO₂H together produces a remarkable cooperative effect on RuO₄⁻, resulting in a much more efficient oxidant. DFT calculations show that Ca²⁺ and CH₃CO₂H can bind to two oxo ligands to form a chelate ring. This results in substantial lowering of the barrier for hydrogen atom abstraction from cyclohexane.

Received 27th July 2020
Accepted 20th October 2020

DOI: 10.1039/d0sc04069j

rsc.li/chemical-science

Introduction

High-valent metal oxo (M=O) complexes are common oxidants in the chemical laboratory and in biological systems. Brønsted acids have long been used to increase the oxidizing power of M=O *via* protonation of the oxo ligand (M=O + HX → M–OH⁺ + X⁻). However, in recent years, the use of Lewis acids (LA) such as metal ions and boranes to activate M=O has received tremendous attention (M=O + LA → M=O–LA).^{1–3} In particular, the interest in understanding the interaction of Lewis acids with metal oxos is stimulated by the discovery that the oxygen-evolving center (OEC) of photosystem II (PSII) is composed of a CaMn₃O₄ cubane and a dangling Mn linked *via* two μ-oxos.^{4–10} A possible role of Ca²⁺ is to function as a Lewis acid to modulate the redox reactivity of the manganese oxo complexes.

Strong Lewis acids such as BF₃ and Sc³⁺ are usually used to activate metal oxo species. For example, we have reported that the oxidation of alkanes by MnO₄⁻ is accelerated by over seven orders of magnitude in the presence of BF₃.¹¹ The strong Lewis acid Sc³⁺ and the strong Brønsted acid CF₃SO₃H have been used

to activate Fe(IV) and Mn(IV) oxo complexes,^{12,13} as well as metal superoxo species.^{14,15}

There is also much interest in the use of the relatively weak Lewis acid, Ca²⁺, to activate M=O because of its relevance to the CaMn₄O₅ cluster in Photosystem II; although as expected, its effect is usually much smaller than those of Sc³⁺ or BF₃. For example, Agapie *et al.* reported that Ca²⁺ and other metal ions can increase the reduction potentials (*E*⁰) of manganese oxo clusters, and there is a linear correlation between *E*⁰ and p*K*_a of the metal ions.^{16,17} Ca²⁺ can also enhance the catalytic water oxidation activity of manganese oxides^{18,19} and induce the oxidative release of O₂ from a non-heme iron peroxo complex.²⁰ We have also recently reported that Ca²⁺ can increase the rate of oxidation of alcohols by MnO₄⁻ (ref. 21) and induce intermolecular O–O coupling of FeO₄²⁻ to give O₂.²² So far, significant activating effects of Ca²⁺ are only reported on metal oxo complexes that are thermodynamically strong oxidants. On the other hand, there has been little or no report on the activation of metal oxo species by weak Brønsted acids such as alkanolic acids.

We have been investigating the effects of Lewis acids on the reactivity of simple metal oxo species bearing two or more oxos without bulky ancillary ligands.^{11,21–25} In this type of systems, more than one oxo sites are available for binding to two or more metal ions or Brønsted acids. We report herein the activation of a stable metal oxo complex, RuO₄⁻, by weak Lewis acids such as Ca²⁺ and other group II ions, as well as by weak Brønsted acids such as CH₃CO₂H. Although iron oxo complexes are common oxidants in chemical and biological systems, they are usually relatively unstable. Hence, we choose to investigate a very stable ruthenium oxo species. Although in a high oxidation state of

^aDongguan Cleaner Production Technology Center, School of Environment and Civil Engineering, Dongguan University of Technology, Dongguan, Guangdong 523808, China

^bDepartment of Chemistry, Jinan University, Guangzhou, 510632, China

^cDepartment of Chemistry, City University of Hong Kong, Tat Chee Avenue, Kowloon Tong, Hong Kong, China. E-mail: bhtclau@cityu.edu.hk; kaichung@cityu.edu.hk; chikmak6@cityu.edu.hk

† Electronic supplementary information (ESI) available. See DOI: 10.1039/d0sc04069j



+VII, RuO_4^- is a mild oxidant that readily oxidizes alcohols but is inactive towards alkanes. However, in the presence of a few equiv. of group 2 metal ions or acetic acid, it readily oxidizes cyclohexane at ambient conditions. Notably, the use of Ca^{2+} and $\text{CH}_3\text{CO}_2\text{H}$ together produces a remarkable cooperative effect on RuO_4^- , resulting in a much more efficient oxidant than the use of a strong Lewis acid in the presence or absence of a Brønsted acid.

Results and discussion

Effects of Lewis acids on oxidation of cyclohexane by $\text{Ru}^{\text{VIII}}\text{O}_4$ and $\text{Ru}^{\text{VII}}\text{O}_4^-$

Tetraoxo complexes of ruthenium in oxidation states +VIII and +VII are known, with $\text{Ru}^{\text{VIII}}\text{O}_4$ being a much stronger oxidant than $\text{Ru}^{\text{VII}}\text{O}_4^-$. As a comparison, we have initially chosen to study the effects of Brønsted and Lewis acids (metal ions and BF_3) on the oxidation of alkanes by RuO_4 . RuO_4 is a strong oxidant that is known to oxidize alkanes slowly at room temperature.²⁶ In our hands, when RuO_4 (0.01 M) was treated with an excess of cyclohexane (1.0 M) in CH_3CN , 0.2 mol of cyclohexanone/mol of RuO_4 (20 mol%) was produced after 5 h at 23 °C, as analysed by GC and GC/MS (Fig. 1a and Table S1†). No cyclohexanol could be detected. Since we previously reported that the oxidation of alkanes by MnO_4^- is greatly enhanced by just a few equiv. of BF_3 ,¹¹ we attempted to do the same with RuO_4 . However, when BF_3 was added to RuO_4 , no enhancement in the rate of cyclohexane oxidation was observed; on the contrary, a lower yield of cyclohexanone (11 mol%) was obtained (Fig. 1a and Table S1†). We then examined if Ca^{2+} can activate RuO_4 , but virtually no effect on cyclohexane oxidation was observed when a few equiv. of $\text{Ca}(\text{OTf})_2$ ($\text{OTf} = \text{CF}_3\text{SO}_3^-$) was added. We also tried to activate RuO_4 with Brønsted acids such as $\text{CF}_3\text{SO}_3\text{H}$ and $\text{CH}_3\text{CO}_2\text{H}$ (AcOH), but again there were no effects. These results indicate that the oxo ligands in the highly electrophilic RuO_4 have little or no affinity for $\text{CH}_3\text{CO}_2\text{H}$ and various Lewis acids.

On the other hand, RuO_4^- is a much weaker oxidant than RuO_4 ; it is known to oxidize alcohols but not alkanes.²⁷ When we treated $[^n\text{Pr}_4\text{N}][\text{RuO}_4^-]$ with cyclohexane in CH_3CN , no product could be detected after 5 days at 23 °C. Electrospray ionization mass spectrometry (ESI/MS) of the solution after 5 days shows that RuO_4^- and $^n\text{Pr}_4\text{N}^+$ are the only species present.

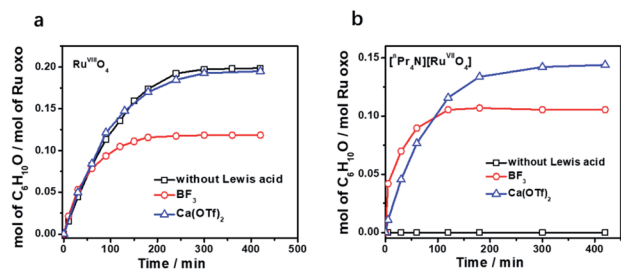
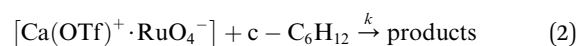
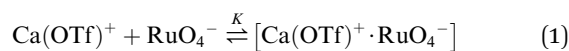


Fig. 1 Time traces for cyclohexane oxidation by (a) $\text{RuO}_4/\text{Lewis acid}$ and (b) $\text{RuO}_4^-/\text{Lewis acid}$ in CH_3CN . Conditions: RuO_4 or $[^n\text{Pr}_4\text{N}][\text{RuO}_4^-]$ (0.01 M), Lewis acid (0.04 M), cyclohexane (1.0 M) at 23 °C.

The UV/Vis spectrum of the solution also remained unchanged after 5 days. However, upon adding 4 equiv. of BF_3 to $[^n\text{Pr}_4\text{N}][\text{RuO}_4^-]$ in CH_3CN , 10 mol% of cyclohexanone was produced within 3 h at 23 °C (Fig. 1b and Table S2†). Again, no cyclohexanol product could be detected. More significantly, $\text{Ca}(\text{OTf})_2$ is also able to activate RuO_4^- , and a higher yield of 14 mol% of cyclohexanone was attained (Fig. 1b, S1 and Table S2†). As will be described below, the $\text{RuO}_4^-/\text{Ca}^{2+}$ system functions as one-electron oxidant, and since the oxidation of cyclohexane to cyclohexanone is a four-electron process, the actual yield is 56%. Other group II metal ions were also found to activate RuO_4^- , with cyclohexanone production ranging from 11 to 15 mol% (Fig. 2, Table S2†). The relatively strong Lewis acid $\text{Sc}(\text{OTf})_3$ was also used and it gave the highest amount of 23 mol% of cyclohexanone. The rate and yield decrease in the order of Sc^{3+} ($\text{p}K_a = 4.3$) > Mg^{2+} (11.2) > Ca^{2+} (12.7) > Sr^{2+} (13.2) >> Ba^{2+} (13.4); this trend correlates with their $\text{p}K_a$ values in H_2O , which is a measure of their Lewis acidity.²⁸ These results indicate that the oxo ligands in RuO_4^- are much more basic than those in RuO_4 , so they readily bind to Lewis acids. Electron-withdrawing by the Lewis acids *via* the oxo ligand enhances the oxidizing power of RuO_4^- .

Kinetics of the oxidation of cyclohexane by $\text{RuO}_4^-/\text{Ca}^{2+}$

The initial rate for cyclohexanone production by $[^n\text{Pr}_4\text{N}][\text{RuO}_4^-]$ increases with $[\text{Ca}^{2+}]$ but eventually levels off at $[\text{Ca}^{2+}] > 5 \text{ mM}$ (Fig. 3a). A plot of $1/(\text{initial rate})$ versus $1/[\text{Ca}(\text{OTf})_2]$ is linear (Fig. 3b). In addition, when the concentration of RuO_4^- was doubled, the initial rate was also doubled. Such a kinetic behavior can be represented by eqn (1) and (2). The reacting calcium species is proposed to be $\text{Ca}(\text{OTf})^+$, as supported by results of DFT calculations described below. The initial rate of the reaction is shown in eqn (3).



$$\text{Initial rate} = \frac{kK[\text{Ca}(\text{OTf})_2]}{1 + K[\text{Ca}(\text{OTf})_2]} [\text{RuO}_4^-][\text{c} - \text{C}_6\text{H}_{12}] \quad (3)$$

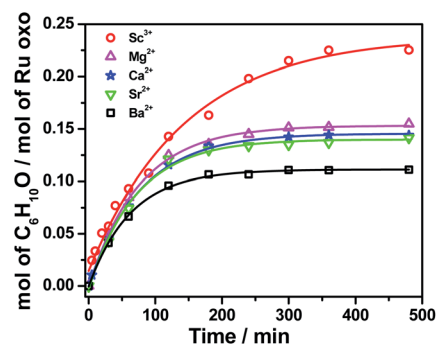


Fig. 2 Effects of various Lewis acids on cyclohexane oxidation by RuO_4^- in CH_3CN . Conditions: $[^n\text{Pr}_4\text{N}][\text{RuO}_4^-]$ (0.01 M), Lewis acid (0.04 M), cyclohexane (1.0 M) at 23 °C.



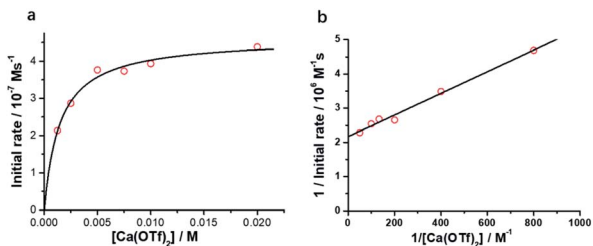


Fig. 3 Effects of $[\text{Ca}(\text{OTf})_2]$ on cyclohexane oxidation by RuO_4^- in CH_3CN . Conditions: $[\text{Pr}_4\text{N}][\text{RuO}_4]$ (0.01 M), cyclohexane (1.0 M) in CH_3CN at 23 °C. (a) Plot of initial rate vs. $[\text{Ca}(\text{OTf})_2]$. (b) Plot of $1/\text{initial rate}$ vs. $1/[\text{Ca}(\text{OTf})_2]$ (slope = $(3.16 \pm 0.15) \times 10^3$, y-intercept = $(2.16 \pm 0.06) \times 10^6$, $r = 0.988$).

From Fig. 3b, $k = 1/(\text{intercept } [\text{RuO}_4^-]) = (4.63 \pm 0.13) \times 10^{-5} \text{ M}^{-1} \text{ s}^{-1}$ and $K = \text{intercept/slope} = (6.83 \pm 0.18) \times 10^2 \text{ M}^{-1}$ at 23 °C. The observed equilibrium constant K indicates relatively strong binding of $\text{Ca}(\text{OTf})_2^+$ to RuO_4^- , in accordance with the observed rate saturation behaviour.

Activation of RuO_4^- by Brønsted acids

The effects of Brønsted acids on cyclohexane oxidation by RuO_4^- were also investigated. Addition of 1 equiv. of the strong acid $\text{CF}_3\text{SO}_3\text{H}$ ($\text{p}K_a = 0.23$ in H_2O) to $[\text{Pr}_4\text{N}][\text{RuO}_4]$ (0.01 M) in CH_3CN containing excess cyclohexane led to the formation of 15 mol% of cyclohexanone after 3 h at 23 °C. However, addition of ≥ 4 equiv. of $\text{CF}_3\text{SO}_3\text{H}$ to $[\text{Pr}_4\text{N}][\text{RuO}_4]$ resulted to rapid formation of a black precipitate with only a trace amount of cyclohexanone. Such a phenomenon is due to disproportionation of RuO_4^- , as represented by eqn (4).²⁹



Interestingly, $[\text{Pr}_4\text{N}][\text{RuO}_4]$ is also readily activated by the relatively weak acid $\text{CH}_3\text{CO}_2\text{H}$ ($\text{p}K_a = 4.76$) to oxidize cyclohexane to cyclohexanone, with no evidence of disproportionation even in the presence of high concentrations of AcOH (>1 M). Upon addition of 12–48 equiv. of AcOH to $[\text{Pr}_4\text{N}][\text{RuO}_4]$ in CH_3CN containing excess cyclohexane, the brown solution gradually turned green, and 16 mol% of cyclohexanone was produced within 1–2 h at 23 °C. The oxidation state of the ruthenium product was determined to be +6 (see below, Fig. S2†), hence the actual yield is 64%. Although the yield is independent of $[\text{AcOH}]$, the rate of oxidation increases with increasing $[\text{AcOH}]$ (Fig. 4); a plot of the initial rate versus $[\text{AcOH}]$ gives a straight line. The initial rate is also doubled when $[\text{RuO}_4^-]$ is doubled. A proposed reaction scheme is shown in eqn (5)–(7). The first step involves protonation of an oxo ligand of RuO_4^- by AcOH , this step is supported by DFT calculations described below. The resulting $[\text{Ru}(\text{O})_3(\text{OH})]$ species is hydrogen-bonded to a second AcOH molecule to generate the active intermediate $[\text{AcOH} \cdot \text{Ru}(\text{O})_3(\text{OH})]$ that oxidizes cyclohexane. The rate law is shown in eqn (8); at $K'[\text{CH}_3\text{CO}_2\text{H}] \ll 1$, the rate law becomes that of eqn (9).

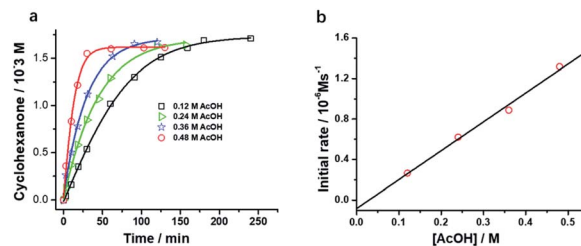
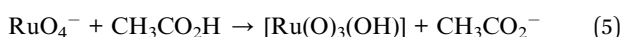
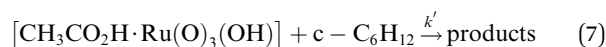
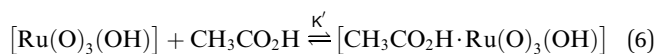


Fig. 4 (a) Effects of $\text{CH}_3\text{CO}_2\text{H}$ on cyclohexane oxidation by RuO_4^- in CH_3CN . Conditions: $[\text{Pr}_4\text{N}][\text{RuO}_4]$ (0.01 M), cyclohexane (1.0 M) in CH_3CN at 23 °C. (b) Plot of initial rate versus $[\text{AcOH}]$ (slope = $(2.72 \pm 0.13) \times 10^{-6}$, y-intercept = $-(3.33 \pm 3.82) \times 10^{-8}$, $r = 0.9908$).



$$\text{Initial rate} = \frac{k'K'[\text{CH}_3\text{CO}_2\text{H}]}{1 + K'[\text{CH}_3\text{CO}_2\text{H}]} [\text{RuO}_4^-][\text{c-C}_6\text{H}_{12}] \quad (8)$$

$$\text{At } K'[\text{CH}_3\text{CO}_2\text{H}] \ll 1$$

$$\text{Initial rate} = k'K'[\text{AcOH}][\text{RuO}_4^-][\text{c-C}_6\text{H}_{12}] = k_{\text{AcOH}}[\text{AcOH}][\text{RuO}_4^-][\text{c-C}_6\text{H}_{12}] \quad (9)$$

From the slope of Fig. 4b and using $[\text{RuO}_4^-] = 0.01 \text{ M}$ and $[\text{c-C}_6\text{H}_{12}] = 1.0 \text{ M}$, k_{AcOH} is found to be $(2.72 \pm 0.13) \times 10^{-4} \text{ M}^{-2} \text{ s}^{-1}$ at 23 °C.

Cooperative activating effects of metal ions and AcOH

Remarkably, when the oxidation of cyclohexane by RuO_4^- was carried out in the presence of Ca^{2+} and AcOH , both the rate and product yield were enhanced, as shown in Fig. 5. The amount of cyclohexanone produced by the $\text{RuO}_4^-/\text{Ca}^{2+}/\text{AcOH}$ system is 38 mol%, compared with ca. 16 mol% by both $\text{RuO}_4^-/\text{Ca}^{2+}$ and $\text{RuO}_4^-/\text{AcOH}$ systems. In this case, the oxidation state of the ruthenium product was found to be +5 (see below, Fig. S3†), so this system functions as a two-electron oxidant and the actual yield is 76%, higher than the 64% using Ca^{2+} or AcOH alone.

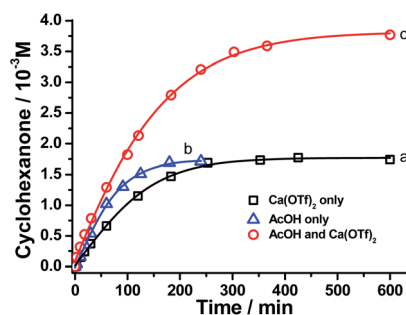
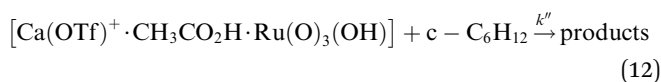
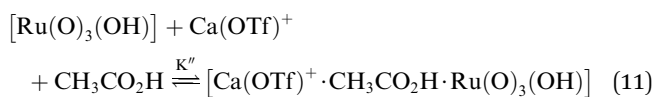
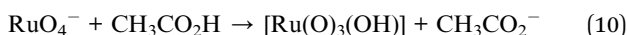


Fig. 5 Time trace for cyclohexane oxidation by $[\text{Pr}_4\text{N}][\text{RuO}_4]$ (0.01 M) in CH_3CN at 23 °C in the presence of (a) 1 equiv. Ca^{2+} , (b) 12 mol equiv. of AcOH and (c) 1 mol equiv. Ca^{2+} + 12 mol equiv. AcOH .



The yield of cyclohexanone was increased to 92% when the amount of acetic acid was increased to 250 equiv. ($\text{CH}_3\text{CN}/\text{AcOH}$: 6/1, Table 1). Note that in the absence of $\text{Ca}(\text{OTf})_2$, the yield of cyclohexanone did not increase with $[\text{AcOH}]$, as illustrated in Fig. 4a. Similar cooperative effects of M^{2+} and AcOH were also found for other group 2 ions (Table 1), with a maximum yield of 99% observed for $\text{Sr}^{2+}/\text{AcOH}$. However, no such cooperative effects were found for stronger Lewis acids such as BF_3 and $\text{Sc}(\text{OTf})_3$, the yields remain the same in the absence or presence of AcOH. These results demonstrate the strong cooperative effects of relatively mild Brønsted and Lewis acid in activating a metal oxo species. Although the reaction rate is lower than that of BF_3 or $\text{Sc}(\text{OTf})_3$, the Group 2 ion/AcOH combination is much more efficient in terms of product yield. Similar to the case of $\text{CF}_3\text{SO}_3\text{H}$ discussed above, partial decomposition of RuO_4^- occurs in the presence of a strong Lewis acid, hence resulting in lower yields.

The kinetics of cyclohexane oxidation by $\text{RuO}_4^-/\text{Ca}^{2+}/\text{AcOH}$ were investigated. Saturation kinetics were also observed when $[\text{Ca}^{2+}]$ was increased (Fig. 6). Based on Fig. 6 and the mechanisms proposed above for $\text{RuO}_4^-/\text{Ca}^{2+}$ and $\text{RuO}_4^-/\text{AcOH}$, the mechanism for this system can be represented by the following equations.



The rate-law is as shown in eqn (13):

$$\text{Initial rate} = \frac{k''K''[\text{Ca}(\text{OTf})_2]}{1 + K''[\text{Ca}(\text{OTf})_2]} [\text{RuO}_4^-][\text{AcOH}][\text{c} - \text{C}_6\text{H}_{12}] \quad (13)$$

Table 1 Oxidation of cyclohexane by $[\text{Pr}_4\text{N}][\text{RuO}_4]/\text{Lewis acid}$ in $\text{CH}_3\text{CN}/\text{AcOH}$ (6:1, v/v)^a

Entry ^a	Lewis acid	Yield of cyclohexanone ^d (%)	Time
1	$\text{Ca}(\text{OTf})_2$	92	5 h
2 ^b	$\text{Ca}(\text{OTf})_2$	92	5 h
3 ^c	$\text{Ca}(\text{OTf})_2$	91	5 h
4	$\text{Sr}(\text{OTf})_2$	99	5 h
5	$\text{Mg}(\text{OTf})_2$	86	5 h
6	$\text{Ba}(\text{OTf})_2$	86	5 h
7	BF_3	42	3 min
8	$\text{Sc}(\text{OTf})_3$	46	6 min

^a Conditions: $[\text{Pr}_4\text{N}][\text{RuO}_4]$, 0.01 M; Lewis acid, 0.04 M; cyclohexane, 1.0 M; solvent, $\text{CH}_3\text{CN}/\text{HOAc}$ (6:1, v/v); at 23 °C. ^b Under argon. ^c In the presence of 10 equiv. of BrCCl_3 , only a trace amount of bromocyclohexane was detected. ^d Yield of cyclohexanone was calculated based on $[\text{Pr}_4\text{N}][\text{RuO}_4]$ acting as two-electron oxidant. Yield = (mol of cyclohexanone)/(mol of $[\text{Pr}_4\text{N}][\text{RuO}_4]$) \times 2 \times 100%, no cyclohexanol was detected.

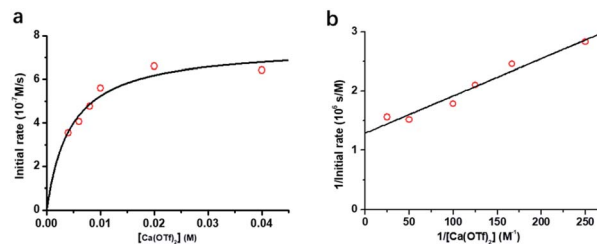


Fig. 6 (a) Plot of initial rate vs. $[\text{Ca}^{2+}]$ for the $\text{Ca}(\text{OTf})_2/\text{AcOH}$ activated oxidation of cyclohexane (0.10 M) by RuO_4^- (0.01 M) in CH_3CN at 23.0 °C. (b) The corresponding plot of $1/\text{initial rate}$ vs. $1/[\text{Ca}^{2+}]$. Slope = $(6.29 \pm 0.64) \times 10^3$, y -intercept = $(1.29 \pm 0.09) \times 10^6$, $r = 0.9504$. Conditions: RuO_4^- (0.01 M); cyclohexane (1.0 M); AcOH (0.12 M); $\text{Ca}(\text{OTf})_2$ (0.002 M – 0.040 M).

From eqn (11) and Fig. 6b, K'' and k'' are found to be $(2.05 \pm 0.31) \times 10^2 \text{ M}^{-1}$ and $(6.49 \pm 0.45) \times 10^{-4} \text{ M}^{-1} \text{ s}^{-1}$, respectively.

A similar cooperative effect was also found for $\text{Mg}^{2+}/\text{AcOH}$ (Fig. S4[†]). However, no increase in rate and yield were found for $\text{Sc}^{3+}/\text{AcOH}$ (Fig. S5[†]).

Ruthenium intermediates and products

Electrospray ionization mass spectrometry (ESI/MS) was employed to detect any intermediate formed between RuO_4^- and Ca^{2+} . The mass spectrum of $[\text{Pr}_4\text{N}][\text{RuO}_4]$ in CH_3CN exhibits a single peak at m/z 166.1 due to RuO_4^- (Fig. S6[†]). Upon addition of 0.25 equiv. of $\text{Ca}(\text{OTf})_2$, a new peak at m/z 653.9 appeared, which is assigned to $[\text{RuO}_4 \cdot \text{Ca}(\text{CF}_3\text{SO}_3)_2 \cdot \text{CF}_3\text{SO}_3\text{H}]^-$ (Fig. S7[†]). MS/MS of this ion (m/z 653.9) gives fragment peaks due to CF_3SO_3^- (m/z 148.9) and RuO_4^- ($m/z = 165.9$) (Fig. S8[†]). This result provides evidence for the binding of Ca^{2+} to RuO_4^- .

The brown color of the solution of $[\text{Pr}_4\text{N}][\text{RuO}_4]/\text{Ca}(\text{OTf})_2$ gradually lightened during cyclohexane oxidation, eventually a dark brown precipitate was observed and the solution became colorless. The dark precipitate, which is probably a Ca^{2+} -bridged polymeric species, was dissolved in 0.1 M HNO_3 and the solution was titrated spectrophotometrically with the strong oxidant $(\text{NH}_4)_2\text{Ce}(\text{NO}_3)_6$ ($\text{Ce}(\text{IV})$). Upon addition of $\text{Ce}(\text{IV})$ to the ruthenium product solution, the characteristic vibronic-structured peaks at around 380 nm due to RuO_4 appeared,²⁶ and 2.3 ± 0.3 equiv. of $\text{Ce}(\text{IV})$ was consumed (Fig. S2[†]). This result indicates that the oxidation state of Ru in the dark brown product is +6 and hence the $\text{Ca}^{2+}/\text{RuO}_4^-$ system acts as one-electron oxidant in the reaction with cyclohexane.

In cyclohexane oxidation by $[\text{Pr}_4\text{N}][\text{RuO}_4]/\text{AcOH}$, the brown solution gradually turned dark green but no precipitate was observed. ESI/MS of the dark green solution shows the appearance of a peak at m/z 209 (Fig. S9[†]), which can be assigned to $[\text{Ru}^{\text{VI}}\text{O}_3(\text{AcO})]^-$. When $\text{CH}_3\text{CO}_2\text{H}$ was replaced by $\text{CD}_3\text{CO}_2\text{D}$, the m/z 209 peak was shifted to m/z 212, indicating that the m/z 209 peak consists of 1 AcO⁻ ion. The assignment of +6 oxidation state to the ruthenium product is also supported by $\text{Ce}(\text{IV})$ titration, which consumes two equiv. of $\text{Ce}(\text{IV})$ to generate RuO_4 . Hence the $\text{RuO}_4^-/\text{AcOH}$ system also functions a one-electron oxidant.



On the other hand, spectrophotometric titration of the product solution of $\text{Ca}^{2+}/\text{AcOH}/\text{RuO}_4^-$ after cyclohexane oxidation shows that it consumes 3.1 ± 0.2 equiv. of $\text{Ce}(\text{IV})$, hence in this case the oxidation state of the Ru product is +5 and the system is a two-electron oxidant towards cyclohexane (Fig. S3†).

Mechanistic studies

The same results were obtained for cyclohexane oxidation carried out under argon or air (Tables 1 and S2†). Also, the addition of BrCCl_3 , a radical scavenger, had little effects on the oxidation of cyclohexane, and only a trace amount of bromocyclohexane was detected (Tables 1 and S2†). These results indicate that no freely diffusing alkyl radicals are formed in the oxidation of cyclohexane by RuO_4^- in the presence of Ca^{2+} and/or AcOH .

The kinetic isotope effects (KIE) for cyclohexane oxidation by RuO_4^- under various conditions were determined by competitive oxidation of an equimolar mixture of $\text{c-C}_6\text{H}_{12}$ and $\text{c-C}_6\text{D}_{12}$. The KIE for $\text{RuO}_4^-/\text{Ca}^{2+}$, $\text{RuO}_4^-/\text{AcOH}$ and $\text{RuO}_4^-/\text{Ca}^{2+}/\text{AcOH}$ were found to be 6.4 ± 0.2 , 13.9 ± 0.4 and 6.5 ± 0.2 , respectively. Such large KIEs are indicative of C–H bond cleavage in the rate-limiting step.

Based on the experimental results, the oxidation of alkane by RuO_4^- in the presence of Lewis acid (LA) appears to be consistent with a mechanism that involves the initial binding of LA to RuO_4^- to generate a precursor complex, which then reacts with alkane *via* a H-atom abstraction/O-rebound mechanism to generate the corresponding alcohol. Such a mechanism is commonly accepted for C–H bond activation by cytochrome P450 and various metal oxo species.³⁰ However, since only ketones are detected in the present case, this suggests that the initially formed alcohol is rapidly oxidized to give the ketone. This is supported by a competitive experiment involving the oxidation of a mixture of cyclohexane and cyclopentanol (10:1) by $\text{RuO}_4^-/\text{Ca}^{2+}$, which resulted in the rapid and exclusive formation of cyclopentanone (Fig. S10†). No alkene or products derived from its oxidation were observed in the oxidation of alkane by $\text{RuO}_4^-/\text{Ca}^{2+}$, which rules out a dehydrogenation mechanism that has been shown to occur in alkane oxidation by non-heme iron(IV) oxo species.³¹ The binding of a Lewis acid to RuO_4^- enhances its oxidizing power, as observed in non-heme iron(IV) oxo complexes³² and manganese oxo clusters.^{16,17}

Theoretical calculations

In order to obtain further insights into the activating effects of $\text{Ca}(\text{II})$ and AcOH on RuO_4^- , the reaction mechanisms for the oxidation of cyclohexane catalysed by RuO_4^- in the presence of $\text{Ca}(\text{OTf})_2$ and/or AcOH have been theoretically studied by density functional theory (DFT). As a comparison similar studies with RuO_4 have also been carried out.

In the oxidation of cyclohexane by $[\text{RuO}_4]^-$ in CH_3CN (Fig. 7), cyclohexane and $[\text{RuO}_4]^-$ first form an intermediate, $\text{INT1}(\text{RuO}_4^-)$, in which the two species are weakly attracted together ($[\text{RuO}_4 \cdots \text{C}_6\text{H}_{12}]^-$). HAT then occurs from C_6H_{12} to $\text{Ru}=\text{O}$ *via* a transition state $\text{TS1}(\text{RuO}_4^-)$ to form a second intermediate, $\text{INT2}(\text{RuO}_4^-)$. The reaction barrier (ΔG_{298}^\ddagger) for

the HAT is $26.8 \text{ kcal mol}^{-1}$ in CH_3CN . Such a large ΔG_{298}^\ddagger agrees with the experimental observation that RuO_4^- hardly reacts with cyclohexane at room temperature. The C1 of the cyclohexyl radical in $\text{INT2}(\text{RuO}_4^-)$ bears -0.93 electrons, consistent with a HAT process. The cyclohexyl radical then binds to another oxo ligand to generate an alkoxo intermediate $[\text{RuO}_2(\text{OH})(\text{OC}_6\text{H}_{11})]^-$ *via* $\text{TS2}(\text{RuO}_4^-)$. It should be noted that the step after H-abstraction is not characterized as a rebound step, in contrast to cytochrome P_{450} and other mono-oxo species. Rather, another oxo group which is not used for H-atom abstraction combines with the carbon atom with a low barrier. Because of this reactivity pattern, a ruthenium-bound alkoxide instead of alcohol is formed as an intermediate. Then in the next step, proton transfer from $\text{Ru}-\text{OH}$ to the alkoxide occurs *via* $\text{TS3}(\text{RuO}_4^-)$ to generate the cyclohexanol product. Similar reaction pathways are observed for cyclohexane oxidation by RuO_4 , except in this case no radical intermediate (INT2) is formed (Fig. S11†). The reaction barrier (ΔG_{298}^\ddagger) is $17.8 \text{ kcal mol}^{-1}$, consistent with the experimental observation that RuO_4 reacts readily with cyclohexane at room temperature.

In the oxidation of cyclohexane by RuO_4^- in the presence of $[\text{Ca}(\text{OTf})]^+$, the reaction mechanism is similar. $[\text{Ca}(\text{OTf})]^+$ forms an intermediate, $\text{INT1}(\text{CaOTf})$, with RuO_4^- ; the Ca is bound to two oxo ligands. Due to the electron withdrawing effects of $\text{Ca}(\text{II})$ centre, the Ru–O bond lengths are changed from 1.740 (in RuO_4^- , Table S3†) to 1.775 (oxo bound to Ca) and 1.709 Å (free oxo) in $\text{INT1}(\text{CaOTf})$. HAT from C_6H_{12} then occurs *via* the shorter and more electrophilic $\text{Ru}=\text{O}$ bond. In this case there is no cyclohexyl radical intermediate, $\text{INT2}(\text{RuO}_4^-)$; HAT and binding of cyclohexyl radical to a second oxo occur in a single step. The ΔG_{298}^\ddagger for the oxidation of cyclohexane by $[\text{RuO}_4(\text{CaOTf})]$ (Fig. 7 and Table S3,† entry 3), *via* $\text{TS1}(\text{CaOTf})$, is $18.5 \text{ kcal mol}^{-1}$. Such a lowering of $8.3 \text{ kcal mol}^{-1}$ is in agreement with the observed accelerating effect of $\text{Ca}(\text{II})$. We have also found the ΔG_{298}^\ddagger for the oxidation of cyclohexane by $[\text{RuO}_4(\text{Ca})]^+$ (Table S3,† entry 5) is higher than that by $[\text{RuO}_4(\text{CaOTf})]$, so $[\text{RuO}_4(\text{Ca})]^+$ should not be the active species in the oxidation of cyclohexane.

In the presence of acetic acid, RuO_4^- is protonated to give $\text{INT1}(\text{AcOH})$, $[\text{RuO}_3\text{OH}(\text{AcO}) \cdots \text{C}_6\text{H}_{12}]$. The AcO^- is held by two additional AcOH molecules through hydrogen bonding (structures given in Table S3†). The Ru–OH bond distance is 1.858 Å; protonation results in shortening of two of the $\text{Ru}=\text{O}$ from 1.740 Å (in RuO_4^-) to 1.709 Å. HAT by $\text{INT1}(\text{AcOH})$ occurs *via* one of the shorter and more electrophilic $\text{Ru}=\text{O}$; the resulting cyclohexyl radical then binds to $\text{Ru}-\text{OH} \cdots \text{OAc}$ to generate Ru bound cyclohexanol in the same step, $\text{INT2}(\text{AcOH})$. The ΔG_{298}^\ddagger for HAT from C_6H_{12} to $\text{INT1}(\text{AcOH})$ *via* $\text{TS1}(\text{AcOH})$ is $15.2 \text{ kcal mol}^{-1}$, which is significantly lower than the ΔG_{298}^\ddagger for RuO_4^- alone by $11.6 \text{ kcal mol}^{-1}$, in accordance with the experimentally observed accelerating effects of AcOH on RuO_4^- .

In the presence of both $[\text{CaOTf}]^+$ and AcOH , the intermediate with RuO_4^- , $\text{INT1}(\text{CaOTf} + \text{AcOH})$, consists of AcO^- and Ca forming a chelate ring with $\text{Ru}=\text{O}$ and $\text{Ru}-\text{OH}$, as well as three H-bonded AcOH molecules (Fig. 7 and Table S3,† entry 4). The free $\text{Ru}=\text{O}$ bonds are further shortened to 1.692 Å. Accordingly



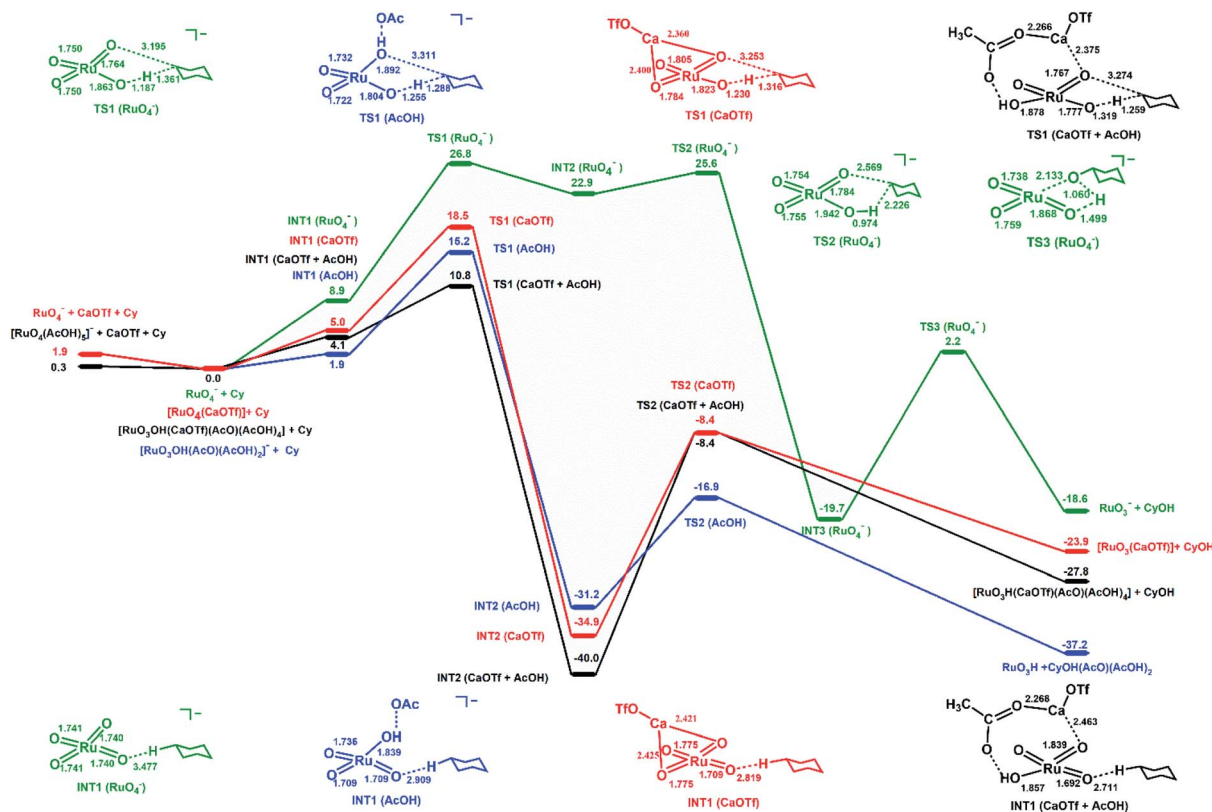


Fig. 7 PESs for cyclohexane oxidation by $[\text{RuO}_4]^-/[\text{RuO}_4(\text{AcOH})]^-/[\text{RuO}_4(\text{CaOTf})]/[\text{RuO}_4(\text{AcOH})(\text{CaOTf})]$ at the B3LYP level using LanL2TZ(f) basis set (Ru) and 6-311++G(d,p) basis set (non-metals). Relative 298 K Gibbs free energies in acetonitrile are given in kcal mol^{-1} . Not all acetic acid molecules are shown for simplicity.

the ΔG_{298}^\ddagger for HAT from cyclohexane *via* $\text{TS1}(\text{CaOTf} + \text{AcOH})$ is lowered to $10.8 \text{ kcal mol}^{-1}$, which is smaller than the value of $18.5 \text{ kcal mol}^{-1}$ and $15.2 \text{ kcal mol}^{-1}$, respectively, with $\text{Ca}(\text{OTf})^+$ or AcOH alone. This is in agreement with the observed cooperative activating effects of AcOH and $\text{Ca}(\text{II})$. HAT and binding of the resulting cyclohexyl radical to a Ca-bound oxo ligand occur in one step. Protonation by Ru–OH to the alkoxide then occurs to generate cyclohexanol. The potential energy surfaces (PES) for $\text{RuO}_4/\text{Ca}(\text{OTf})^+$, RuO_4/AcOH and $\text{RuO}_4/\text{Ca}(\text{OTf})^+/\text{AcOH}$ are shown in Fig. S11.† The ΔG_{298}^\ddagger for HAT by RuO_4 alone is $17.8 \text{ kcal mol}^{-1}$, consistent with the experimental observation that RuO_4 is able to oxidize cyclohexane at ambient conditions. There are little or no changes in the Ru=O distances of RuO_4 upon binding to $\text{Ca}(\text{OTf})^+$ and/or AcOH , and there are only small changes in the reaction barriers, in agreement with experimental observations. This is in accordance with the Ru=O bonds being highly electrophilic and non-basic, hence there is little affinity for Lewis acids.

Conclusions

Our results demonstrate a remarkable cooperative effect of a weak Brønsted acid and a weak Lewis acid on the activation of a metal oxo species. RuO_4^- , although in high oxidation state of +VII, is a weak oxidant due to stabilization by the four oxo ligands. However, it can be readily activated by a mild Lewis

acid such as Ca^{2+} or other group II metal ions, as well as a weak Brønsted acid such as $\text{CH}_3\text{CO}_2\text{H}$. The addition of both Ca^{2+} and $\text{CH}_3\text{CO}_2\text{H}$ generates a highly efficient system that can oxidize unactivated C–H bonds with much higher yields than the use of strong Lewis acids such as Sc^{3+} or BF_3 , with or without $\text{CH}_3\text{CO}_2\text{H}$. Such an observation may provide insights into the design of active oxidants based on metal oxo species in combination with relatively weak Brønsted and Lewis acids, especially if the metal oxo or the substrate is sensitive to strong acids. Our studies may also be relevant to oxidation by metal oxo species in biological systems, where only mild Brønsted acids such as alkanolic or amino acids, and mild Lewis acids such as Zn^{2+} or Ca^{2+} , are present in cells. So may be highly efficient oxidizing systems can be generated in biological systems using this strategy.

Conflicts of interest

There are no conflicts to declare.

Acknowledgements

This work was supported by the Hong Kong Research Grants Council (CityU 11336816), the National Science Foundation of China (21975043) and Guangdong Provincial Key Platforms and Major Scientific Research Projects for Colleges and Universities



(2018KTSCX227). We thank Dr Hajime Hirao for very helpful discussions.

Notes and references

- 1 T. Devi, Y.-M. Lee, W. Nam and S. Fukuzumi, *Coord. Chem. Rev.*, 2020, **410**, 213219.
- 2 Y. Liu and T.-C. Lau, *J. Am. Chem. Soc.*, 2019, **141**, 3755–3766.
- 3 S. Fukuzumi, *Coord. Chem. Rev.*, 2013, **257**, 1564–1575.
- 4 D. J. Vinyard, G. M. Ananyev and G. C. Dismukes, *Annu. Rev. Biochem.*, 2013, **82**, 577–606.
- 5 J. Yano and V. Yachandra, *Chem. Rev.*, 2014, **114**, 4175–4205.
- 6 J. D. Blakemore, R. H. Crabtree and G. W. Brudvig, *Chem. Rev.*, 2015, **115**, 12974–13005.
- 7 J. Barber, *Chem. Soc. Rev.*, 2009, **38**, 185–196.
- 8 Y. Umena, K. Kawakami, J.-R. Shen and N. Kamiya, *Nature*, 2011, **473**, 55–60.
- 9 K. M. Davis, B. T. Sullivan, M. C. Palenik, L. Yan, V. Purohit, G. Robison, I. Kosheleva, R. W. Henning, G. T. Seidler and Y. Pushkar, *Phys. Rev. X*, 2018, **8**, 041014.
- 10 Y. Pushkar, K. M. Davis and M. C. Palenik, *J. Phys. Chem. Lett.*, 2018, **9**, 3525–3531.
- 11 W. W. Y. Lam, S.-M. Yiu, J. M. N. Lee, S. K.-Y. Yau, H.-K. Kwong, T.-C. Lau, D. Liu and Z. Lin, *J. Am. Chem. Soc.*, 2006, **128**, 2851–2858.
- 12 Y. Morimoto, H. Kotani, J. Park, Y.-M. Lee, W. Nam and S. Fukuzumi, *J. Am. Chem. Soc.*, 2011, **133**, 403–405.
- 13 H. Yoon, H. Yoon, Y.-M. Lee, X. Wu, K.-B. Cho, R. Sarangi, W. Nam and F. S. Fukuzumi, *J. Am. Chem. Soc.*, 2013, **135**, 9186–9194.
- 14 T. Devi, Y.-M. Lee, W. Nam and S. Fukuzumi, *J. Am. Chem. Soc.*, 2020, **142**, 365–372.
- 15 T. Devi, Y.-M. Lee, W. Nam and S. Fukuzumi, *J. Am. Chem. Soc.*, 2018, **140**, 8372–8375.
- 16 E. Y. Tsui, R. Tran, J. Yano and T. Agapie, *Nat. Chem.*, 2013, **5**, 293–299.
- 17 E. Y. Tsui and T. Agapie, *Proc. Natl. Acad. Sci. U.S.A.*, 2013, **110**, 10084–10088.
- 18 M. M. Najafpour, T. Ehrenberg, M. Wiechen and P. Kurz, *Angew. Chem., Int. Ed.*, 2010, **49**, 2233–2237.
- 19 M. Wiechen, I. Zaharieva, H. Dau and P. Kurz, *Chem. Sci.*, 2012, **3**, 2330–2339.
- 20 S. Bang, Y.-M. Lee, S. Hong, K.-B. Cho, Y. Nishida, M. S. Seo, R. Sarangi, S. Fukuzumi and W. Nam, *Nat. Chem.*, 2014, **6**, 934–940.
- 21 H. Du, Po-K. Lo, Z. Hu, H. Liang, K.-C. Lau, Y.-N. Wang, W. W. Y. Lam and T.-C. Lau, *Chem. Commun.*, 2011, **47**, 7143–7145.
- 22 L. Ma, W. W. Y. Lam, P.-K. Lo, K.-C. Lau and T.-C. Lau, *Angew. Chem., Int. Ed.*, 2016, **55**, 3012–3016.
- 23 T.-C. Lau and C.-K. Mak, *J. Chem. Soc., Chem. Commun.*, 1993, 766–767.
- 24 S.-M. Yiu, Z.-B. Wu, C.-K. Mak and T.-C. Lau, *J. Am. Chem. Soc.*, 2004, **126**, 14921–14929.
- 25 S.-M. Yiu, W.-L. Man, X. Wang, W. W. Y. Lam, S.-M. Ng, H.-K. Kwong, K.-C. Lau and T.-C. Lau, *Chem. Commun.*, 2011, **47**, 4159–4161.
- 26 W. P. Griffith, *Ruthenium Oxidation Complexes: Their Uses as Homogenous Organic Catalysts*, Springer, 2011.
- 27 W. P. Griffith, S. V. Ley, G. P. Whitcombe and A. D. White, *J. Chem. Soc., Chem. Commun.*, 1987, 1625–1627.
- 28 S. J. Hawkes, *J. Chem. Educ.*, 1996, **73**, 516.
- 29 E. A. Seddon and K. R. Seddon, *The Chemistry of Ruthenium*, Elsevier, Amsterdam, 1984, vol. 52.
- 30 J. L. McLain, J. Lee and J. T. Groves, *Biomimetic Oxidations Catalyzed by Transition Metal Complexes*. Imperial College Press, London, 2000.
- 31 K.-B. Cho, X. Wu, Y.-M. Lee, Y. H. Kwon, S. Shaik and W. Nam, *J. Am. Chem. Soc.*, 2012, **134**, 20222–20225.
- 32 W. Nam, Y.-M. Lee and S. Fukuzumi, *Acc. Chem. Res.*, 2014, **47**, 1146–1154.

